

Biomimetic synthesis of Ag/TiO₂ nanocomposites using a natural surfactant for effective degradation of an environmental pollutant

DOI: 10.25177/JESES.5.2.RA.10604

Short Communication

Accepted Date: 15th March 2020; Published Date: 20th March 2020

Copy rights: © 2020 The Author(s). Published by Sift Desk Journals Group
This is an Open Access article distributed under the terms of the Creative Commons Attribution License (<http://creativecommons.org/licenses/by/4.0/>), which permits unrestricted use, distribution, and reproduction in any medium, provided the original work is properly cited.

Pravat Manjari Mishra^{a*}; Santosh Kumar Sahoo^a; Deepak Kumar Padhi^a

^aEnvironment and Sustainability Department, CSIR-Institute of Minerals and Materials Technology, Bhubaneswar-751013, Odisha

CORRESPONDENCE AUTHOR

Pravat Manjari Mishra

Email: pravatmanjari@yahoo.co.in or pravatmanjari@immt.res.in

CITATION

Pravat Manjari Mishra, Biomimetic synthesis of Ag/TiO₂ nanocomposites using a natural surfactant for effective degradation of an environmental pollutant(2020)Journal of Earth Sciences & Environmental Studies 5(2) pp:44-50

ABSTRACT

The present paper involves the synthesis of bio-based Ag/TiO₂ nanocomposites using both dry and fresh leaf extracts of *Averrhoa carambola* L. as reducing, capping and stabilizing agents. The nanocomposites are characterized by UV-vis DRS, XRD, TEM and EDX spectroscopy. TEM analysis shows the formation of somewhat uniformly distributed AgNPs on the surface of TiO₂. From the UV-vis DRS studies and band gap energy calculation, it is confirmed that Ag/TiO₂ DLE is more active than Ag/TiO₂ FLE. The photocatalytic activity of the Ag/TiO₂ nanocomposites prepared by both the leaf extracts was studied towards the degradation of methyl orange (MO). It was found that both FLE and DLE induced Ag/TiO₂ exhibited higher efficiency towards photocatalytic degradation of MO as compared to chemically prepared Ag/TiO₂. It was observed that DLE induced Ag/TiO₂ exhibited higher efficiency towards photocatalytic degradation of MO as compared to FLE induced Ag/TiO₂.

Keywords: Biomimetic; Nanocomposites; *Averrhoa carambola* L.; photocatalytic activity.

1. INTRODUCTION

The unconsumed dyes and toxic chemicals present in the industrial effluents are now the subjects of considerable concern of environmental remediation. Noble metal-doped metal oxide nanocomposites are considered as the areas of great research for the degradation of these environmental pollutants due to their high oxidation activity, good thermal stability and selectivity. Some nanocomposites showed excellent results towards environmental remediation [1-10].

Among them, Ag/TiO₂ system is of immense importance and has been a subject of interest in the field of photocatalytic degradation of environmental pollutants. Khan et al. studied the photodecomposition of methylene blue (MB) in an aqueous solution using synthesized Ag-TiO₂ nanocomposites under visible light irradiation [11]. The excellent photocatalytic degradation efficiency of Ag-TiO₂ microwires were studied by Mandal and Bhattacharyya, 2012 [12]. Nainani et al. studied the photocatalytic efficiency of Ag-TiO₂ towards degradation of methyl orange [13]. Enhancement in the photocatalytic oxidation of oxalic acid by silver deposition on a TiO₂ surface is studied by Szabó-Bárdos et al. [14].

But the chemical methods which are employed for the synthesis of Ag/TiO₂ nanocomposites, involve the use of harmful toxic chemicals. Thus environmental friendly processes need to be adopted for the synthesis of these nanocomposites. Jiang et al., 2013 synthesized two-dimensional TiO₂@Ag heterojunction structure using edible corn cripsey, which exhibited efficient photocatalytic activity towards the degradation of methylene blue (MB) [15]. Au/TiO₂ and Ag/TiO₂ composites synthesized using Citrus limon plant extracts, showed excellent photocatalytic activity towards degradation of organic dye [16]. But very less literature is available on the synthesis of Ag/TiO₂ composites by biomimetic approaches. Earlier, we have reported the synthesis of Au/TiO₂ using aqueous leaf extract of *C. tamala* and its remarkable photocatalytic activity towards the degradation of MO [17].

In the present study, we have first time used aqueous leaf extract (both dry and fresh leaf extract) of *Aver-*

rhoa carambola L. (Order Oxalidales, family Oxalidaceae) for the biomimetic synthesis of Ag/TiO₂ nanocomposites. The biomolecules such as reducing sugar, proteins, flavonoids and mainly the carambolaflavone present in the leaf extracts act as reducing, capping and stabilizing agents in the synthesis Ag/TiO₂ nanocomposites [18, 19]. The biosynthesized Ag/TiO₂ composites showed remarkable photocatalytic activity towards degradation of MO.

2. MATERIALS AND METHODS

2.1 Materials and chemicals used

AgNO₃, H₂SO₄ (0.01 M), NaOH (0.01 N) and C₂H₅OH (absolute) were purchased from NICE chemicals Pvt. Ltd, Qualigens, Rankem and Merck respectively.

2.2 Preparation of aqueous leaf extract (LE)

FLE (Fresh leaf extract) was prepared by boiling 10 g of thoroughly washed fresh leaves of *A. carambola* with 100 mL of de-ionised water at 50°C for 30 min. and filtered through Whatman 1 filter paper. DLE (Dry leaf extract) was prepared by boiling 2 g of shade-dried leaf powder with 100 mL of ultrapure water at 50°C for 15 min and filtered.

2.3 Preparation of 2 wt% Ag/TiO₂ nanocomposite

1 gm of Degussa P-25 TiO₂ was mixed with 20 mL of distilled water in a beaker and stirred for 30 mins. 187 mL of 1 mM AgNO₃ solution (0.02g Ag) was added dropwise for 2 hrs with vigorous stirring. The pH of the resulting suspension was maintained to 5.5 to 5.6 by adding 0.01 N NaOH solution. Then 47 mL of aqueous LE (equivalent to ¼ th of AgNO₃ solution used-since this concentration was found to be appropriate from spectroscopic and kinetic studies, Fig. 1) was added at a time to suspension and stirred for 4 hrs vigorously. The colour of the suspension was changed from white to brown and then it was centrifuged. The residue was washed for two times with DI water followed by centrifugation. Finally, the residue was washed with ethanol and centrifuged to collect the residue. The residue was dried overnight in an incubator at 30°C. Then, the residue was subjected to calcination in a muffle furnace for 4 hrs at 450°C at a rising temperature rate of 5°C/min. The two cata-

lysts prepared by the above method are labeled as Ag/TiO₂-FLE and Ag/TiO₂-DLE. Similarly, Ag/TiO₂-C is prepared using NaBH₄ as reducing agent in place of LE.

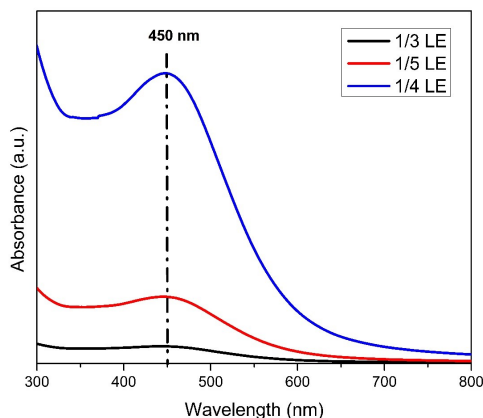
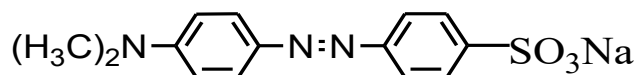


Fig. 1 DRS UV-Visible spectra of AgNPs varying the concentration of leaf extract

2.4 Photocatalytic activity

The photocatalytic activity of the catalysts was evaluated by the photocatalytic degradation of MO in aqueous solution. The photocatalysis was performed in sunlight during 10:00 am to 2:00 pm in sunny days of March.



Methyl Orange

The photocatalytic degradation of MO was carried out by taking 20 ml of 100 mg/l MO solution in a 100 ml flask, over 1.0 g/l of catalyst. The solution was exposed to sunlight with constant stirring. In all cases, the mixture was kept in the dark for 30 minutes to ensure that the adsorption-desorption equilibrium was reached before irradiation. After visible light irradiation, the sample was withdrawn from the suspension at every 60 minutes during irradiation for the determination of change in absorbance of MO. The catalyst was removed by centrifugation and MO content in the solution was analyzed quantitatively by light absorption at 464 nm.

2.5 Characterization

The nanocomposites were characterized by UV-Vis

spectrophotometer (Jasco V-650), XRD (X'Pert Pro P Analytical X-ray diffractometer), TEM technique (Phillips, TECNAI FEI G² TEM operating at 200Kv) equipped with EDX attachment.

3. RESULTS AND DISCUSSION

3.1 DRS UV-Visible analysis

From the DRS UV-visible spectra of the samples (Fig. 2 A), it was found that the absorption spectra of Ag/TiO₂ nanocomposites synthesized by both DLE and FLE, were shifted towards the visible region and this might be responsible for the enhancement of photocatalytic activity under solar radiation. Significantly enhanced absorption spectra in the visible region of longer wavelength at 500-600 nm are due to SPR effect of metallic AgNPs. The strong absorption at 200-340 nm is characteristic of TiO₂. The enhanced absorbance intensity of Ag/TiO₂ synthesized by DLE than that of Ag/TiO₂ synthesized by FLE confirmed that more no of AgNPs are synthesized by DLE than FLE.

The band gap energy of TiO₂, Ag/TiO₂ DLE, Ag/TiO₂ FLE were calculated by the Tauc approach using the equation 1 and shown in (Fig. 2 B) [20].

$$ah\nu = A(h\nu - E_g)^n \quad [1]$$

Where a= absorption coefficient

ν = light frequency

A = proportionality constant

E_g = band gap energy

n= Type of transition in a semiconductor.

It is a direct transition if $n = \frac{1}{2}$ and indirect transition for $n = 2$. Here the value of n for all the synthesized compounds was taken as 1/2, which confirms that optical transition of nanocomposites are directly allowed [20]. The band gap energy of all the composites are approximated from the plot of $(ah\nu)^n$ vs $h\nu$ by extrapolating the straight line to the X axis intercept. The band gap energies of TiO₂, Ag/TiO₂ FLE, Ag/TiO₂ DLE were found to be 3.12, 2.98, 2.90 eV respectively (Fig. 2 B). The low band gap of Ag/TiO₂ DLE and Ag/TiO₂ FLE nanocomposites indicates that they have tendency towards visible light motivated photocatalytic ability.

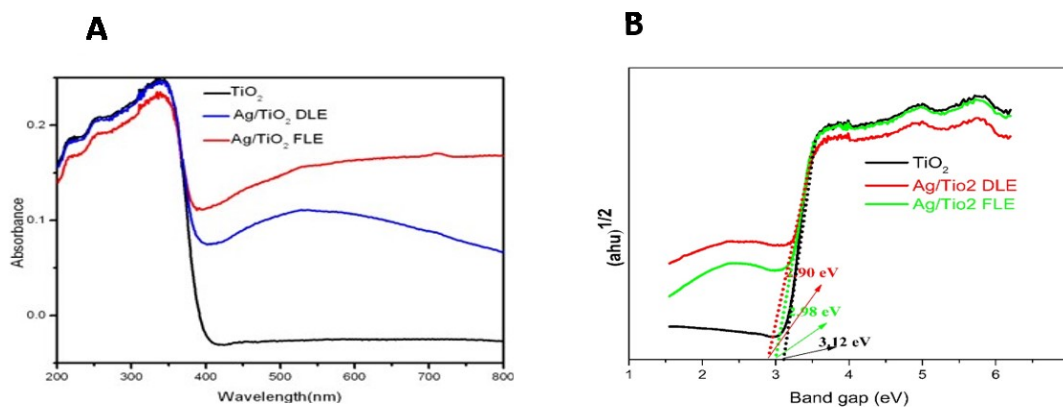


Fig. 2 (A) DRS UV-Visible spectra of TiO_2 and Ag/TiO_2 nanocomposites; (B) Estimated bandgap energy for TiO_2 , Ag/TiO_2 -DLE, Ag/TiO_2 -FLE nanocomposites.

3.2 XRD Analysis

For pure TiO_2 all peaks are well indexed as the anatase phase (JCPDS card No. 83-2243). The XRD patterns of Ag/TiO_2 nanocomposites (Fig. 3) almost coincide with that of pure TiO_2 , and no diffraction peaks is observed for Ag, thus suggesting that the metal particles are well dispersed on the surface of TiO_2 . Ag/TiO_2 nanocomposites did not show any peak shift, indicating that the TiO_2 matrix was well maintained as the anatase phase which indicates that the metal dopants are merely placed on the surface of the crystals without being covalently bonded into the crystal lattice. The presence of Ag on TiO_2 is also confirmed by EDX spectra which detected Ag element. The average crystalline sizes were calculated by Scherrer equation and found to be 72.29 nm and

76.17 nm for FLE and DLE induced Ag/TiO_2 nanocomposites respectively.

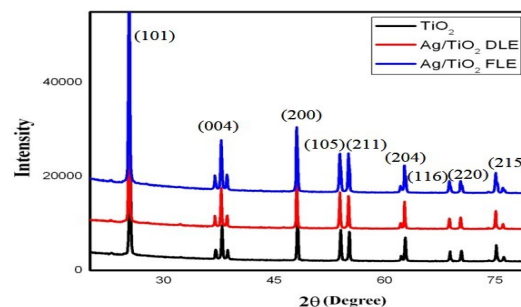


Fig. 3 XRD pattern of TiO_2 and Ag/TiO_2 nanocomposites

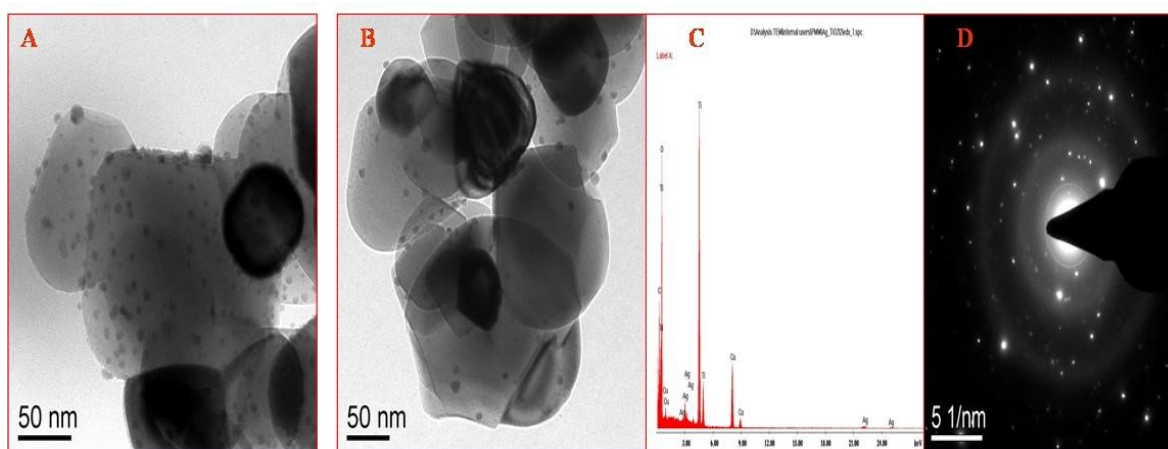


Fig. 4 (A) represents TEM image of Ag/TiO_2 nanocomposite synthesized by FLE; (B) represents TEM image of Ag/TiO_2 nanocomposite synthesized by DLE; (C) represents EDX of Ag/TiO_2 nanocomposite; (D) shows its SAED pattern.

3.3 TEM analysis

The synthesized Ag/TiO₂ nanocomposites were characterized by TEM which shows somewhat uniformly distributed AgNPs on titania (Fig. 4). TEM micrographs show a variation of AgNPs size in the range of 1-13 nm. The average particle size of AgNPs was found to be less than 10 nm in the case of both DLE and FLE induced NPs. The presence of silver was confirmed by EDX spectroscopy.

3.4 Photocatalytic activity

The photocatalytic activity of Ag/TiO₂-FLE, Ag/TiO₂-DLE and Ag/TiO₂-C nanocomposites were tested for the degradation of MO in sunlight. The result of the MO degradation by the catalysts was presented in Fig. 5 A. From the study, it was found that Ag/TiO₂-DLE exhibited higher efficiency towards photocatalytic degradation of MO than Ag/TiO₂-FLE, whereas chemically prepared Ag/TiO₂-C exhibited less photocatalytic activity in comparison to all. In 30 min. of reaction time, Ag/TiO₂-DLE showed 67.2% degradation of MO, whereas Ag/TiO₂-FLE showed 53.7% of MO degradation. The percentage of degradation of MO increases with an increase in time in the case of all the catalysts. In 3 hr, the percentages of degradation of MO by Ag/TiO₂-DLE, Ag/TiO₂-FLE and Ag/TiO₂-C were 78.85, 72.9 and 63.2, respectively. The enhanced catalytic activity of Ag/TiO₂-DLE than that of Ag/TiO₂-FLE confirmed that the more number of AgNPs are synthesized in Ag/TiO₂-DLE than in Ag/TiO₂-FLE. This is because more number of phytoconstituents of *A. carambola* leaves are available in DLE

than FLE. More the number of biomolecules, stronger the interaction between biomolecules and the nanoparticles. The biomolecules act both as reducing and stabilizing agents for synthesis of more AgNPs. The AgNPs are capped with the biconstituents of *A. carambola* and the agglomeration between AgNPs is prevented.

With an increase in no. of AgNPs, in the case of Ag/TiO₂-DLE, the catalytic activity is enhanced compared to Ag/TiO₂-FLE, due to the SPR effect of AgNPs. When the Ag/TiO₂ nanocomposites are irradiated (Fig. 5 B) with visible light, the electron from the valance band (VB) of Ag migrates to the conduction band (CB), by absorbing a photon. As a result, the electrons and holes are formed on the surface of the AgNPs. Many researchers reported that due to the SPR effect, the electrons in CB of Ag transferred to the conduction band of TiO₂ [21, 22]. Herein, the electrons generated on the surface of the AgNPs due to the SPR effect, migrated to the CB of TiO₂ and there they get trapped by the adsorbed oxygen molecules leading to the formation of superoxide radicals. These superoxide radicals and the trapped electrons can combine to produce H₂O₂, finally forming hydroxyl radicals. The holes formed on the surface of the AgNPs are trapped by water molecules to produce reactive hydroxyl radicals. Those superoxide radicals and hydroxyl radicals anions (strong oxidants) then oxidize the organic pollutant (MO) on the surface of the nanocomposite.

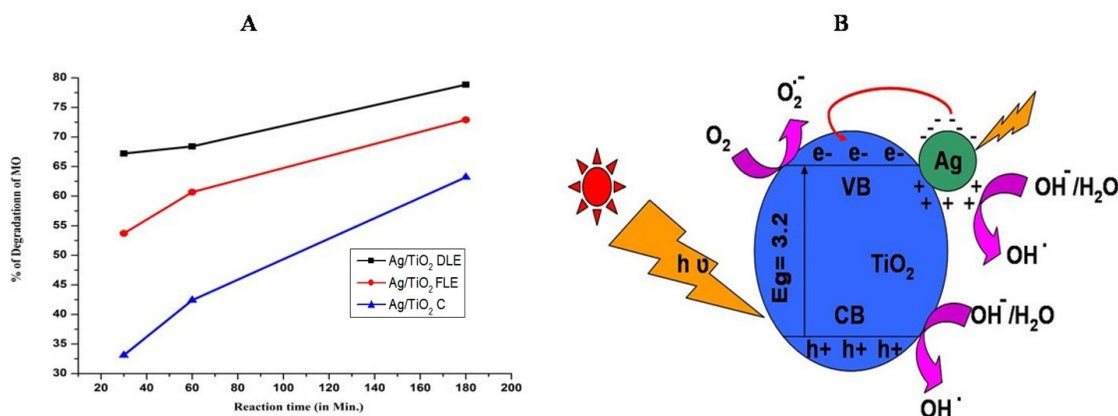


Fig. 5 (A) Degradation of MO using Ag/TiO₂-FLE, Ag/TiO₂-DLE and Ag/TiO₂-C; (B) Schematic diagram of enhanced photocatalytic activity of Ag/TiO₂ nanocomposite

CONCLUSION

This is the first report of the synthesis of Ag/TiO₂ nanocomposites using both DLE and FLE of *A. carmabola*. Ag/TiO₂-DLE exhibited higher efficiency towards photocatalytic degradation of MO as compared to Ag/TiO₂-FLE, due to the synthesis of more number of AgNPs by DLE than FLE, which is also evident from UV-Vis DRS studies of both the nanocomposites as well as from the estimated bandgap energy of Ag/TiO₂-DLE, Ag/TiO₂-FLE nanocomposites (Fig. 2 A & B). These biosynthesized Ag/TiO₂ nanocomposites have shown comparable or higher photocatalytic activities towards degradation of MO in comparison to chemically prepared Ag/TiO₂-C. This green, simple and cost-effective method could prove to be a better alternative to chemical synthesis methods and also effective for the large scale preparation of stable Ag/TiO₂ nanocomposites.

Acknowledgements

The authors thank Director, CSIR-IMMT, for providing the facilities to carry out this work and CSIR for funding the project.

REFERENCES

- [1] Xu YG, Liu J, Xie M, Jing LQ, Xu H, She XJ, Li HM, Xie JM. Construction of novel CNT/LaVO₄ nanostructures for efficient antibiotic photodegradation. *Chemical Engineering Journal* 2019; 357:487-497. [View Article](#)
- [2] Xu Y, Liu Q, Liu C, Zhai Y, Xie M, Huang L, Xu H, Li H, Jing J. Visible-light-driven Ag/AgBr/ZnFe₂O₄ composites with excellent photocatalytic activity for *E. coli* disinfection and organic pollutant degradation. *Journal of Colloid and Interface Science* 2017, 512:555-566 PMid:29100160 [View Article](#) [PubMed/NCBI](#)
- [3] Tian Y, Zhou L, Zhu Q, Lei J, Wang L, Zhang J, Liu Y. Hierarchical macro-mesoporous g-C₃N₄ with an inverse opal structure and vacancies for high-efficiency solar energy conversion and environmental remediation. *Nanoscale* 2019, 11:20638-20647. PMid:31641721 [View Article](#) [PubMed/NCBI](#)
- [4] Hunge YM, Yadav AA, Dhodamani AG, Suzuki N, Terashima C, Fujishima A, Mathe VL. Enhanced photocatalytic performance of ultrasound treated GO/TiO₂ composite for photocatalytic degradation of salicylic acid under sunlight illumination. *Ultrasonics sonochemistry* 2020, 61:104849. PMid:31710997 [View Article](#) [PubMed/NCBI](#)
- [5] Hunge YM, Yadav AA, Liu S, Mathe VL. Sonochemical synthesis of CZTS photocatalyst for photocatalytic degradation of phthalic acid. *Ultrasonics sonochemistry* 2019, 56:284-289. PMid:31101264 [View Article](#) [PubMed/NCBI](#)
- [6] Hunge YM, Yadav AA, Mathe VL. Oxidative degradation of phthalic acid using TiO₂ photocatalyst. *Journal of Materials Science: Materials in Electronics* 2018, 29:6183-6187. [View Article](#)
- [7] Ali T, Hunge YM, Venkatraman A. UV assisted photoelectrocatalytic degradation of reactive red 152 dye using spray deposited TiO₂ thin films. *Journal of Materials Science: Materials in Electronics* 2018, 29:1209-1215. [View Article](#)
- [8] Hunge YM. Sunlight assisted photoelectrocatalytic degradation of benzoic acid using stratified WO₃/TiO₂ thin films. *Ceramics International* 2017, 43:10089-10096. [View Article](#)
- [9] Hunge YM, Yadav AA, Mohite BM, Mathe VL. Photoelectrocatalytic degradation of sugarcane factory wastewater using WO₃/ZnO thin films. *Journal of Materials Science: Materials in Electronics* 2018, 29:3808-3816. [View Article](#)
- [10] Yadav AA, Hunge YM, Mathe VL, Kulkarni SB. Photocatalytic degradation of salicylic acid using BaTiO₃ photocatalyst under ultraviolet light illumination. *Journal of Materials Science: Materials in Electronics* 2018, 29:5069-15073. [View Article](#)
- [11] Khan MM, Ansari SA, Amal MI, Lee J, Cho MH. Highly visible light active Ag@TiO₂ nanocomposites synthesized using an electrochemically active biofilm: a novel biogenic approach. *Nanoscale* 2013; 5:4427-4435. PMid:23579384 [View Article](#) [PubMed/NCBI](#)
- [12] Mandal SS, Bhattacharyya AJ. Electrochemical sensing and photocatalysis using Ag-TiO₂ mi-

- crowires. *J. Chem. Sci.* 2012, 124:969-978. [View Article](#)
- [13] Nainani R, Thakur P, Chaskar M. Synthesis of silver doped TiO₂ nanoparticles for the improved photocatalytic degradation of methyl orange. *Journal of Materials Science and Engineering B* 2012; 2:52-58.
- [14] Szabó-Bárdos E, Czili H, Horváth A. Photocatalytic oxidation of oxalic acid enhanced by silver deposition on a TiO₂ surface. *Journal of Photochemistry and Photobiology A: Chemistry* 2003, 154:195-201. 00330-1 [View Article](#)
- [15] Jiang B, Hou Z, Tian C, Zhou W, Zhang X, Wu A, Tian G, Pan K, Ren Z, Fu H (2013) A facile and green synthesis route towards two-dimensional TiO₂@Ag heterojunction structure with enhanced visible light photocatalytic activity. *Cryst. Eng. Comm.* 2013; 15(29):5821-5827. [View Article](#)
- [16] Liang W, Church TL, Harris AT (2012) Biogenic synthesis of photocatalytically active Ag/TiO₂ and Au/TiO₂ composites. *Green. Chem.* 2012; 14:968-975. [View Article](#)
- [17] Naik GK, Mishra PM, Parida K. Green synthesis of Au/TiO₂ for effective dye degradation in aqueous system. *Chemical Engg. Journal* 2013; 299:492-497. [View Article](#)
- [18] Dasgupta P, Chakraborty P, Bala NN. Avertroha Carambola: An Updated Review. *Int. J. Pharm. Res. Rev.* 2013; 2(7):54-63.
- [19] Mishra PM, Sahoo SK, Naik GK, Parida K. Biomimetic synthesis, characterization and formation mechanism of stable silver nanoparticles using Avertroha carambola L. leaf extract. *Materials Letters* 2015, 160:566-571. [View Article](#)
- [20] D. K. Padhi, K. Parida. Facile fabrication of α -FeOOH nanorod/RGO composite: a robust photocatalyst for reduction of Cr(VI) under visible light irradiation. *J. Mater. Chem. A.* 2014, 2:10300-10312. [View Article](#)
- [21] Chen Z, Fang L, Dong W, Zheng F, Shen M, Wang J. Inverse opal structured Ag/TiO₂ plasmonic photocatalyst prepared by pulsed current deposition and its enhanced visible light photocatalytic activity. *J. Mater. Chem. A* 2014; 2:824-832. [View Article](#)
- [22] Wang P, Tang Y, Dong Z, Chen Z, Lim TT. Ag-AgBr/TiO₂/RGO nanocomposite for visible-light photocatalytic degradation of penicillin G. *J. Mater. Chem A* 2013; 1:4718-4727. [View Article](#)